PERGAMON

International Journal of Heat and Mass Transfer 45 (2002) 4267–4279

International Journal of HEAT and MASS TRANSFER

www.elsevier.com/locate/ijhmt

Solution of an initial-boundary value problem for heat conduction in a parallelepiped by time partitioning

David H.Y. Yen [a], James V. Beck [b], Robert L. McMasters [c,*], Donald E. Amos [d]

[a] *Department of Mathematics, Michigan State University, East Lansing, MI 48824, USA*
[b] *Department of Mechanical Engineering, Albuquerque, NM 87110, USA*
[c] *Department of Mechanical Engineering, Michigan State University, East Lansing, MI 48824, USA*
[d] *Sandia National Laboratories (Retired), Albuquerque, NM 87110, USA*

Received 6 June 2001; received in revised form 6 April 2002

Abstract

An initial-boundary value problem for transient heat conduction in a rectangular parallelepiped is studied. Solutions for the temperature and heat flux are represented as integrals involving the Green's function (GF), the initial and boundary data, and volumetric energy generation. Use of the usual GF obtained by separation of variables leads to slowly convergent series. To circumvent this difficulty, the dummy time interval of integration is partitioned into a short time and a long time subintervals where the GFs are approximated by their small and large time representations. This paper deals with the analysis and implementation of this time partitioning method. © 2002 Elsevier Science Ltd. All rights reserved.

1. Introduction

Accurate and efficient computation of transient heat conduction problems are needed for the verification [5,6] of numerical methods such as the finite difference, finite element and boundary element methods. Of particular interest are three-dimensional problems, such as in a rectangular parallelepiped. The temperature and the three heat flux components are needed, all to considerable accuracy. Obtaining such solutions using classical methods, such as separation of variables, can be difficult. A classic procedure for linear nonhomogeneous boundary conditions is to reduce the problem to one having homogeneous boundary conditions for the transient part of the solution and the nonhomogeneous conditions treated in a related steady state problem. This procedure is powerful but sometimes does not yield satisfactory answers for the temperature. Results for the heat flux are even worse.

An example of evaluation problems using classical methods can be demonstrated by using a steady state solution given in Carslaw and Jaeger [3]. This solution is for prescribed temperature on all six faces of a rectangular parallelepiped. One simple case is for a unit cube with one surface at a constant nonzero temperature and the remaining five surfaces at zero temperature. The solution can be used to derive the normal heat flux at the center point of the surface with a nonzero temperature. As the number of terms in the double summations increases, the heat flux oscillates between approximately -1.5 and 6 in dimensionless units. The methods described in this paper do not present such ambiguous results and are very efficient.

The methods are based on the use of transient Green's functions (GFs). The (GFs, for brevity) are used in integrals for problems involving prescribed boundary and initial conditions and for volumetric energy generation. The GF is denoted $G(x,x',y,y',z,z',t-\tau)$ which for rectangular parallelepipeds can be written as the product of three one-dimensional GFs. (The GF can be considered to be the temperature at the point (x,y,z) and time t for a Dirac delta source at (x',y',z') and time τ.) Two different kinds of GFs are used in the same

* Corresponding author. Tel.: +1-517-332-2712; fax: +1-517-353-1750.
E-mail address: mcmaste7@msu.edu (R.L. McMasters).

0017-9310/02/$ - see front matter
PII: S0017-9310(02)00145-X

Nomenclature

$E(w)$	shorthand notation for the function $E(w) = \mathrm{erfc}(w/(4\alpha u)^{1/2})$
G	Green's function
H	overall body length in the y dimension (m)
k	thermal conductivity (W/mK)
$K(w,u)$	shorthand notation for the function $K(w,u) = 2(\pi u\alpha)^{-1/2}\exp(-w^2/4\alpha u)$
L	overall body length in the x dimension (m)
q_x	heat flux in the x direction $q_x = -k\partial T/\partial x$ (W/m^2)
r_1	another expression for y
r_2	another expression for $W - y$
r_3	another expression for z
r_4	another expression for $H - z$
t	time (s)
t_p	partition time (s)
$S(y,u)$	shorthand notation for $1 - E(y) - E(W - y)$
$S(z,u)$	shorthand notation for $1 - E(z) - E(H - z)$
T	temperature (K)
T^L	long time contribution to the temperature solution (K)
T^S	short time contribution to the temperature solution (K)
T_0	surface temperature at $x = 0$ (K)
u	transformation variable, $u = t - \tau$ (s)
w	generic variable for space (m)
W	overall body length in the z dimension (m)
x, y, z	spatial variables (m)
x', y', z'	dummy variables of integration for space (m)

Greek symbols

α	thermal diffusivity, $\alpha = k/\rho c$ (m^2/s)
β	eigenvalue (m^{-1})
δ	Dirac delta function
τ	dummy variable of integration for time (s)
ω_{mnp}	shorthand notation for eigenvalues $\omega^2_{mnp} = \beta^2_m/L^2 + \beta^2_n/W^2 + \beta^2_p/H^2$

Subscripts

b.c.	boundary condition case
in	initial condition case
g	internal energy generation case
x, y, z	direction of applicability for Green's functions
m, n, p	counting integers for eigenvalues in the x, y and z directions

Superscripts

S	short time temperature or Green's function
L	long time temperature or Green's function

problem by employing the concept of time partitioning. One kind is derived using the method of separation of variables and the other is derived using the Laplace transform. The former kind converges rapidly for "large" $t - \tau$ and the second kind for small $t - \tau$.

To illustrate the method of time partitioning, the following specific problem for a rectangular parallelepiped is studied: The temperature at one of the faces is raised to a nonzero constant value T_0 at time $t = 0$ while the temperature at the other five faces are held at zero. Using the notation in Ref. [2] this problem is denoted X11B10Y11B00Z11B00T0. (The "1" after X, Y and Z denotes boundary conditions of the first kind.) The effects of initial conditions and volumetric energy generation will be considered. We shall determine the temperature and heat fluxes in the parallelepiped, say to nine digit accuracy, by the method of time partitioning.

GFs are used to obtain expressions for the temperature and heat fluxes in the form of integrals involving these GFs $G(x,x',y,y',z,z',t-\tau)$, the initial and boundary data, and volumetric energy generation. Difficulty arises when one wishes to evaluate such integrals as the GFs do not have uniform convergence properties for all τ in the interval $(0,t)$ of integration. To circumvent this difficulty the method of time partitioning is used. The interval of integration $(0,t)$ is partitioned into subintervals $(0,t-t_p)$ and $(t-t_p,t)$ with some partition time parameter $t_p > 0$. Large time (large $t-\tau$) representations for the GFs are used in the subinterval $(0,t-t_p)$ while small time (small $t-\tau$) representations for the GFs are used in $(t-t_p,t)$. The situation is similar to the so-called "Ewald summation" in solid state physics where the electric potential due to a periodic lattice is expressed as a sum of a global Fourier type expansion and an expansion that is local in space. Based on the Ewald summation Strain [8] developed several computational algorithms for steady state potential problems. More recently Linton [4] followed the same idea and developed computational algorithms for other steady state problems. It will be shown in this paper that time partitioning is an accurate and efficient method for transient as well as steady state heat conduction problems.

The time partitioning method is discussed in Refs. [2,5] where the general procedure for multi-dimensional problems is discussed and many short time forms of GFs are tabulated. The discussion in [2] for three-dimensional problems, however, is rather limited and the issues of implementation and the resulting accuracy improvement are not discussed. Ref. [5] gives a framework for the solution of three-dimensional problems

with an emphasis on obtaining precise numerical results but does not concern itself with the analysis and the implementation of the time partitioning method. These issues will be considered here. Thus the present paper may be regarded as a companion to [5] as they are intended to complement each other.

It is not unusual to encounter slowly convergent infinite series representations for GFs in other scientific and engineering disciplines. Electromagnetic scattering problems and water wave theory, for example, provide many such examples. Depending on the circumstances quite often classical techniques such as Kummer's transformation can lead to accelerated convergence of the series [1]. Other techniques include the use of Poisson's summation formula and integral representations. Here in the time partitioning method rapidly convergent series representations are used in different time regimes. No further measures are necessary to accelerate the convergence of the GFs that are used here.

For background materials on heat conduction we refer the readers to [2,3,7]. Refs. [2,3] provides extensive background on the use of GFs in solving heat conduction problems. Both short time and long time GFs are listed in [2,5]. It has served as a benchmark for heat conduction solutions for many years. GFs are briefly addressed in [7], along with other general approaches to solving heat conduction problems.

This paper is organized as follows. In Section 2 we present the formulation of the problem. Section 3 deals with the implementation of the time partitioning method. Short time and long time GFs are introduced in the appropriate integrals which are manipulated analytically. A scheme by which an optimum partition time can be determined is introduced and a method by which the optimum partition time may be estimated is given. The effects of initial condition and volumetric energy generation are studied. Section 4 contains numerical results and discussions, and Section 5 contains the summary and conclusions.

2. Temperature in a rectangular parallelepiped

Consider the region $0 < x < L, 0 < y < W, 0 < z < H$ in the three-dimensional space. The temperature $T(x, y, z, t)$, for constant material properties and in the presence of volumetric heat generation, satisfies the heat equation

$$\frac{\partial^2 T}{\partial x^2} + \frac{\partial^2 T}{\partial y^2} + \frac{\partial^2 T}{\partial z^2} + \frac{1}{k} g(x, y, z, t) - \frac{1}{\alpha} \frac{\partial T}{\partial t} = 0 \tag{1}$$

where k is the thermal conductivity; α, the thermal diffusivity; and $g(x, y, z, t)$, the volumetric energy generation. We impose the initial condition

$$T(x, y, z, 0) = F(x, y, z) \tag{2}$$

and the boundary conditions of

$$\begin{aligned} T(0, y, z, t) = f(y, z, t), \quad T(L, y, z, t) &= T(x, 0, z, t) \\ = T(x, W, z, t) &= T(x, y, 0, t) \\ = T(x, y, H, t) &= 0 \end{aligned} \tag{3}$$

The GF $G(x, x', y, y', z, z', t - \tau)$ for the problem above is governed by

$$\frac{\partial^2 G}{\partial x^2} + \frac{\partial^2 G}{\partial y^2} + \frac{\partial^2 G}{\partial z^2} - \frac{1}{\alpha} \frac{\partial G}{\partial t} = 0, \quad t > \tau \tag{4}$$

with the initial condition at $t = \tau$

$$G(x, x', y, y', z, z', 0) = \delta(x - x')\delta(y - y')\delta(z - z') \tag{5}$$

and the isothermal boundary conditions

$$\begin{aligned} G(0, x', y, y', z, z', t - \tau) &= G(L, x', y, y', z, z', t - \tau) \\ &= G(x, x', 0, y', z, z', t - \tau) \\ &= G(x, x', W, y', z, z', t - \tau) \\ &= G(x, x', y, y', 0, z', t - \tau) \\ &= G(x, x', y, y', H, z', t - \tau) \\ &= 0 \end{aligned} \tag{6}$$

For a homogeneous parallelepiped it is known that $G(x, x', y, y', z, z', t)$ can be expressed as the product of three one-dimensional GFs

$$\begin{aligned} G(x, x', y, y', z, z', t - \tau) = G_X(x, x', t - \tau) G_Y(y, y', t - \tau) \\ \times G_Z(z, z', t - \tau) \end{aligned} \tag{7}$$

where $G_X(x, x', t - \tau)$ satisfies

$$\frac{\partial^2 G_X}{\partial x^2} - \frac{1}{\alpha} \frac{\partial G_X}{\partial t} = 0 \tag{8}$$

$$G_X(x, x', 0) = \delta(x - x') \tag{9}$$

$$G_X(0, x', t) = G_X(L, x', t) = 0 \tag{10}$$

($G_Y(y, y', t - \tau)$ and $G_Z(z, z', t - \tau)$ satisfy similar equations.) Such one-dimensional GFs can be found in [2,5] in various forms.

It is known [2] that the temperature $T(x, y, z, t)$ subject to the initial and boundary conditions given be Eqs. (2) and (3) can be expressed as

$$\begin{aligned} T(x, y, z, t) = T_{\text{b.c.}}(x, y, z, t) + T_{\text{in}}(x, y, z, t) \\ + T_{\text{g}}(x, y, z, t) \end{aligned} \tag{11}$$

where

$$\begin{aligned} T_{\text{b.c.}}(x, y, z, t) = \alpha \int_{\tau=0}^{t} f(y', z', \tau)\, \mathrm{d}\tau \frac{\partial G_X(x, 0, t - \tau)}{\partial x'} \\ \times \int_{y'=0}^{W} \int_{z'=0}^{H} G_Y(y, y', t - \tau) \\ \times G_Z(z, z', t - \tau)\, \mathrm{d}y'\, \mathrm{d}z' \end{aligned} \tag{12}$$

$$T_{\text{in}}(x,y,z,t) = \int_{x'=0}^{L}\int_{y'=0}^{W}\int_{z'=0}^{H} F(x',y',z')G_X(x,x',t) \times G_Y(y,y',t)G_Z(z,z',t)\,\mathrm{d}x'\,\mathrm{d}y'\,\mathrm{d}z' \tag{13}$$

$$T_{\text{g}}(x,y,z,t) = \frac{\alpha}{k}\int_{\tau=0}^{t}\mathrm{d}\tau\int_{x'=0}^{L}\int_{y'=0}^{W}\int_{z'=0}^{H} g(x',y',z',\tau) \times G_X(x,x',t-\tau)G_Y(y,y',t-\tau) \times G_Z(z,z',t-\tau)\,\mathrm{d}x'\,\mathrm{d}y'\,\mathrm{d}z' \tag{14}$$

We note that $T_{\text{b.c.}}(x,y,z,t)$ above represents the temperature due to the nonhomogeneous boundary condition, $T_{\text{in}}(x,y,z,t)$ represents the temperature due to the initial condition, and $T_{\text{g}}(x,y,z,t)$ represents the temperature due to volumetric energy generation.

For general boundary and initial conditions and volumetric energy generation, the above integrals for $T_{\text{b.c.}}$, T_{in}, and T_{g} must be computed numerically. We shall address the question as to how such numerical computations should proceed in general with the method of time partitioning later. Let us now consider the simplified conditions:

$$\begin{aligned} &f(y,z,t) = T_0 = \text{constant}\\ &F(x,y,z) = 0\\ &g(x,y,z,t) = g_0 = \text{constant}\end{aligned} \tag{15}$$

These simplifications enable us to carry out most of our computations analytically and illustrate better how the method of time partitioning works.

Let $u = t - \tau$ we can now rewrite Eqs. (12) and (14) (which respectively solve the problems X11B10Y11B10Z11B10T and X11B00Y11B00Z11B00T0G1)

$$T_{\text{b.c.}}(x,y,z,t) = \alpha T_0\int_{u=0}^{t}\frac{\partial G_X(x,0,u)}{\partial x'}\int_{y'=0}^{W} G_Y(y,y',u)\,\mathrm{d}y' \times \int_{z'=0}^{H} G_Z(z,z',u)\,\mathrm{d}z'\,\mathrm{d}u \tag{16}$$

$$T_{\text{g}}(x,y,z,t) = \frac{\alpha g_0}{k}\int_{u=0}^{t}\int_{x'=0}^{L} G_X(x,x',u)\,\mathrm{d}x' \times \int_{y'=0}^{W} G_Y(y,y',u)\,\mathrm{d}y' \times \int_{z'=0}^{H} G_Z(z,z',u)\,\mathrm{d}z'\,\mathrm{d}u \tag{17}$$

(Notice that $T_{\text{in}}(x,y,z,t)$ now is identically zero.) The corresponding expressions for the heat fluxes are given by the negatives of the spatial derivatives multiplied by k. For example, the heat flux $q_{\text{b.c.}x}(x,y,z,t)$ in the x-direction corresponding to $T_{\text{b.c.}}(x,y,z,t)$ above is given by

$$q_{\text{b.c.}x}(x,y,z,t) = -\alpha k T_0\int_{\tau=0}^{t}\frac{\partial^2 G_X(x,0,u)}{\partial x\,\partial x'} \times \int_{y'=0}^{W} G_Y(y,y',u)\,\mathrm{d}y' \times \int_{z'=0}^{H} G_Z(z,z',u)\,\mathrm{d}z'\,\mathrm{d}u \tag{18}$$

We shall use such expressions for the heat fluxes and present some numerical results later.

3. The method of time partitioning

In this section we shall illustrate the method of time partitioning by considering the computation of $T_{\text{b.c.}}(x,y,z,t)$ given in Eq. (16). For brevity we shall drop the subscripts b.c. The expression involves integration with respect to u from 0 to t. We partition the interval $(0,t)$ into the subintervals $(0,t_{\text{p}})$ and (t_{p},t), where t_{p} is a time partitioning parameter, and use the short time and long time expressions for the GFs in the respective subintervals. We then consider the computational problems.

3.1. Short time and long time Green's functions

In the subinterval for u in $(0,t_{\text{p}})$ the short time GFs may be represented by

$$G_X(x,x',u) \simeq G_X^{\text{S}}(x,x',u) \tag{19}$$

$$G_Y(y,y',u) \simeq G_Y^{\text{S}}(y,y',u) \tag{20}$$

$$G_Z(z,z',u) \simeq G_Z^{\text{S}}(z,z',u) \tag{21}$$

where [2]

$$G_X^{\text{S}}(x,x',u) = \sum_{m=-M}^{M}(K(2mL+x-x',u) - K(2mL+x+x',u)) \tag{22}$$

$$G_Y^{\text{S}}(y,y',u) = \sum_{n=-N}^{N}(K(2nW+y-y',u) - K(2nW+y+y',u)) \tag{23}$$

$$G_Z^{\text{S}}(z,z',u) = \sum_{p=-P}^{P}(K(2pH+z-z',u) - K(2pH+z+z',u)) \tag{24}$$

and

$$K(w,u) = \frac{1}{(4\alpha\pi u)^{1/2}}\exp(-w^2/(4\alpha u)) \tag{25}$$

Exact expressions are recovered as M, N and P are allowed to go to infinity.

The expressions given in Eqs. (22)–(24) can be derived using the method of images or the method of Laplace transforms. These expressions converge rapidly for small $\alpha u/L^2$ as only a few terms are needed for accurate results; that is, M, N and P need be only one or two for accurate values.

In the subinterval for u in (t_p, t) $(t > t_p)$ we have the representations for the GFs obtained by eigenfunction expansions,

$$G_X^L(x,x',u) \simeq \frac{2}{L}\sum_{m=1}^{M} \exp(-\beta_m^2 \alpha u/L^2)\sin\frac{\beta_m x}{L} \times \sin\frac{\beta_m x'}{L} \tag{26}$$

$$G_Y^L(y,y',u) \simeq \frac{2}{W}\sum_{n=1}^{N} \exp(-\beta_n^2 \alpha u/W^2)\sin\frac{\beta_n y}{W} \times \sin\frac{\beta_n y'}{W} \tag{27}$$

$$G_Z^L(z,z',u) \simeq \frac{2}{H}\sum_{p=1}^{P} \exp(-\beta_p^2 \alpha u/H^2)\sin\frac{\beta_p z}{H} \times \sin\frac{\beta_p z'}{H} \tag{28}$$

where $\beta_q = q/\pi$ and M, N and P need not be the same as those in Eqs. (22)–(24). These representations are valid for all u except near $u = 0$, but are most computationally efficient for $\alpha u/L^2$, $\alpha u/W^2$ or $\alpha u/H^2$ not too small.

Let us introduce the functions

$$T_{b.c.}^S(x,y,z,t) = \alpha T_0 \int_0^t \frac{\partial G_X^S(x,0,u)}{\partial x'} \times \int_{y'=0}^{W} G_Y^S(y,y',u)\,dy' \times \int_{z'=0}^{H} G_Z^S(z,z',u)\,dz'\,du, \quad t \leqslant t_p \tag{29}$$

$$T_{b.c.}^L(x,y,z,t,t_p) = \alpha T_0 \int_{t_p}^t \frac{\partial G_X^L(x,0,u)}{\partial x'} \int_{y'=0}^{W} G_Y^L(y,y',u)\,dy' \times \int_{z'=0}^{H} G_Z^L(z,z',u)\,dz'\,du, \quad t > t_p \tag{30}$$

Thus, given t_p, we can write

$$T_{b.c.}(x,y,z,t) = T_{b.c.}^S(x,y,z,t), \quad t \leqslant t_p \tag{31}$$

$$T_{b.c.}(x,y,z,t) = T^S(x,y,z,t_p) + T^L(x,y,z,t,t_p), \quad t > t_p \tag{32}$$

Steady state solutions are obtained by letting t go to infinity in Eq. (32). The expressions in Eqs. (29) and (30) represent respectively the short time and long time contributions to $T_{b.c.}(x,y,z,t)$, which are considered in the next two sections.

3.2. Short time computation

In this section a simple approximation is used. When the series in Eqs. (22)–(24) are substituted into Eq. (29) and are truncated, errors arise due to the y'- and z'-integrations as well as the u-integration. Consider the y'-integration in Eq. (29). Substitute the truncated small time GF G_Y^S

$$G_Y^S(y,y',u) \simeq K(y-y',u) - K(y+y',u) + K(2W-y+y',u) - K(2W-y-y',u) + K(2W+y-y',u) \tag{33}$$

into the y'-integral to obtain

$$\int_{y'=0}^{W} G_Y^S(y,y',u)\,dy' = 1 - E(y) - E(W-y) + E(W+y) + E(2W-y) - \frac{1}{2}(E(2W+y) + E(3W-y)) \tag{34}$$

where

$$E(w) = \operatorname{erfc}\left(\frac{w}{\sqrt{4\alpha u}}\right) \tag{35}$$

and erfc denotes the complementary error function [1]. The function E decays rapidly as $w/(4\alpha u)^{1/2}$ increases. (Notice that $0 < y < W$.) Thus in this simple approximation we truncate the right side of Eq. (34) after the "1" and work with the dimensionless time $\alpha u/W^2$ up to no higher than 0.05 in practice for the short time GFs. Similar arguments can be made for G_Z^S. With the y'- and z'-integrals being replaced by unity we have in essence replaced the three-dimensional problem by a one-dimensional problem for short time.

We now consider the u-integrations for $T_{b.c.}^S(x,y,z,t)$. We take

$$G_X^S(x,x',u) \simeq K(x-x',u) - K(x+x',u) - K(2L-x-x',u) + K(2L-x+x',u) + K(2L+x-x',u) + [K(2L+x+x',u)] \tag{36}$$

(through second reflections). As the source term is taken to be $x' = 0$, the left end of the interval of interest, the reflection at the left end is more significant than that at the right end and there is a rearrangement of the order of magnitude of the terms. Thus it is advantageous to add the extra left reflection term (in brackets) in Eq. (36) which accounts for the third reflection. Substituting Eq. (36) into Eq. (29) and carrying out the x'-differentiation and the u-integration leads to, for $t \leqslant t_p$

$$T^{S}_{b.c.}(x,y,z,t) \simeq T_0 \int_{u=0}^{t} (xK(x,u) - (2L-x)K(2L-x,u) + (2L+x)K(2L+x,u)) \frac{du}{u}$$
$$= T_0 \left(\operatorname{erfc}\left(\frac{x}{\sqrt{4\alpha t}} \right) - \operatorname{erfc}\left(\frac{2L-x}{\sqrt{4\alpha t}} \right) + \operatorname{erfc}\left(\frac{2L+x}{\sqrt{4\alpha t}} \right) \right) \quad (37)$$

For small t and x not near L the first term in Eq. (37) alone provides good approximation

$$T^{S}_{b.c.}(x,y,z,t) \simeq T_0 \operatorname{erfc}\left(\frac{x}{\sqrt{4\alpha t}} \right) \quad (38)$$

which is the one-dimensional solution for a semi-infinite solid.

To account for the three-dimensional effects we include the functions $E(y)$ and $E(W-y)$ and similar functions of z in the y'- and z'-integrations in Eq. (29). We have, instead of Eq. (37),

$$T^{S}_{b.c.}(x,y,z,t) \simeq T_0 \int_{u=0}^{t} (xK(x,u) - (2L-x)K(2L-x,u) + (2L+x)K(2L+x,u)) \times S(y,u)S(z,u) \frac{du}{u} \quad (39)$$

where

$$S(y,u) \simeq 1 - \operatorname{erfc}\left(\frac{y}{\sqrt{4\alpha u}} \right) - \operatorname{erfc}\left(\frac{W-y}{\sqrt{4\alpha u}} \right) \quad (40)$$

$$S(z,u) \simeq 1 - \operatorname{erfc}\left(\frac{z}{\sqrt{4\alpha u}} \right) - \operatorname{erfc}\left(\frac{H-z}{\sqrt{4\alpha u}} \right) \quad (41)$$

Expanding Eq. (39) above and dropping higher order terms leads to

$$T^{S}_{b.c.}(x,y,z,t) \simeq T_0 \left\{ \int_{u=0}^{t} (xK(x,u) - (2L-x)K(2L-x,u) + (2L+x)K(2L+x)) \frac{du}{u} - \int_{u=0}^{t} (xK(x,u) - (2L-x)K(2L-x,u) + (2L+x)K(2L + x)) \sum_{i=1}^{4} \operatorname{erfc}\left(\frac{r_i}{\sqrt{4\alpha u}} \right) \frac{du}{u} + \int_{u=0}^{t} xK(x,u) \times \sum_{i=1}^{2} \sum_{j=3}^{4} \operatorname{erfc}\left(\frac{r_i}{\sqrt{4\alpha u}} \right) \operatorname{erfc}\left(\frac{r_j}{\sqrt{4\alpha u}} \right) \frac{du}{u} \right\} \quad (42)$$

where

$$r_1 = y, \quad r_2 = W - y, \quad r_3 = z, \quad r_4 = H - z \quad (43)$$

We see that for small u and for y not near zero or W and z not near zero or H, $S(y,u)$ and $S(z,u)$ in Eqs. (40) and (41) can both be approximated by unity and hence the short time computation reduces to the one-dimensional expression in Eq. (37). Also, for small u and x not close to L, Eq. (37) further reduces to the well-known result in Eq. (38). Differentiating Eq. (38) with respect to x and setting $x = 0$ leads to

$$q^{S}_{b.c.x}(0,t) = \frac{kT_0}{\sqrt{\pi\alpha t}} \quad (44)$$

Consider the case of small time but for y and z near an edge, say $y = z = 0$. For small y and z we have from Eq. (39) or (42)

$$T^{S}_{b.c.}(x,y,z,t) \simeq T_0 \int_{u=0}^{t} xK(x,u) \times \operatorname{erf}\left(\frac{y}{\sqrt{4\alpha u}} \right) \operatorname{erf}\left(\frac{z}{\sqrt{4\alpha u}} \right) \frac{du}{u} \quad (45)$$

This equation gives the exact solution for the octant $x > 0$, $y > 0$, $z > 0$ with temperature T_0 on $x = 0$ and zero temperature along $y = 0$ and $z = 0$. Differentiating Eq. (45) above with respect to x yields

$$q^{S}_{b.c.x}(x,y,z,t) \simeq -kT_0 \int_{u=0}^{t} K(x,u) \left(1 - \frac{x^2}{2\alpha u} \right) \times \operatorname{erf}\left(\frac{y}{\sqrt{4\alpha u}} \right) \operatorname{erf}\left(\frac{z}{\sqrt{4\alpha u}} \right) \frac{du}{u} \quad (46)$$

In the general case it is possible to pursue the computation analytically using Eq. (42), but we shall omit the details here. Some numerical results on the three-dimensional improvements using Eq. (42) and based on numerical integrations will be reported later in the paper.

3.3. Long time computation

We now return to Eq. (30) for $T^{L}_{b.c.}(x,y,z,t,t_p)$. With the long time GF G^{L}_{Y} and G^{L}_{Z} given in Eqs. (27) and (28) the y'- and z'-integrations can be carried out to get

$$\int_{y'=0}^{W} G^{L}_{Y}(y,y',u)\,dy' = \begin{cases} 4\sum_{n=1}^{N} \frac{1}{\beta_n} \exp(-\beta_n^2 \alpha u / W^2) \sin(\beta_n y / W) & n \text{ odd} \\ 0, & n \text{ even} \end{cases} \quad (47)$$

$$\int_{z'=0}^{H} G^{L}_{Z}(z,z',u)\,dz' = \begin{cases} 4\sum_{p=1}^{P} \frac{1}{\beta_p} \exp(-\beta_p^2 \alpha u / H^2) \sin(\beta_p z / H) & p \text{ odd} \\ 0, & p \text{ even} \end{cases} \quad (48)$$

Performing the u-integration in Eq. (30) now results in

$$T^{\mathrm{L}}_{\mathrm{b.c.}}(x,y,z,t) = \int_{t_\mathrm{p}}^{t} \sum_{m=1}^{M} \sum_{n=1\,\mathrm{odd}}^{N} \sum_{p=1\,\mathrm{odd}}^{P} \times \exp(-\omega^2_{mnp}\alpha u) f_{mnp}(x,y,z)\,\mathrm{d}u = \sum_{m=1}^{M} \sum_{n=1\,\mathrm{odd}}^{N} \sum_{p=1\,\mathrm{odd}}^{P} f_{mnp}(x,y,z) \times \frac{\exp(-\omega^2_{mnp}\alpha t_\mathrm{p}) - \exp(-\omega^2_{mnp}\alpha t)}{\alpha\omega^2_{mnp}} \quad (49)$$

where

$$f_{mnp}(x,y,z) = \frac{32\alpha T_0 \beta_m}{L^2\beta_n\beta_p} \sin(\beta_m x/L)\sin(\beta_n y/W) \times \sin(\beta_p z/H) \quad (50)$$

$$\omega^2_{mnp} = \beta^2_m/L^2 + \beta^2_n/W^2 + \beta^2_p/H^2 \quad (51)$$

It is seen that there are two triple series in Eq. (49) above. The first triple series (associated with t_p in the numerator) is slowly convergent as t_p tends to zero. The terms in the series then decay like $\beta_m/\beta_n\beta_p\omega^2_{mnp}$, i.e., they decay algebraically. The situation becomes even worse when one wishes to compute the heat fluxes, for then the terms are multiplied further by β_m, β_n or β_p through differentiation with respect to x, y or z and the decay becomes even slower, if at all.

The difficulty associated with small t_p above is circumvented by the method of time partitioning in that the short time contribution is treated by the short time GFs. The right-hand side of Eq. (49) converges rapidly for t_p bounded away from zero, owing to the exponential decay of the factors $\exp(-\omega^2_{mnp}\alpha t_\mathrm{p})$ and $\exp(-\omega^2_{mnp}\alpha t)$ for large m, n and p. More specifically, since

$$\mathrm{e}^{-15} = 3.06\mathrm{E}{-7}, \quad \mathrm{e}^{-20} = 2.06\mathrm{E}{-9}, \quad \mathrm{e}^{-23} = 1.03\mathrm{E}{-10} \quad (52)$$

we may, by restricting the arguments in the exponential to an appropriate value, ensure the solution to be at least as accurate as these values. For example, by choosing the argument to be 20 (as done for the computations given below), the error in the values should be less than E−10. Notice that the denominator also reduces the contribution of the larger values of m, n and p.

3.4. The optimum partition time t_p

For a general parallelepiped whose L, W and H may not be all equal, one can have partition times $\alpha t_{\mathrm{p}1}/L^2$, $\alpha t_{\mathrm{p}2}/W^2$ and $\alpha t_{\mathrm{p}3}/H^2$. The parameters $t_{\mathrm{p}1}$, $t_{\mathrm{p}2}$ and $t_{\mathrm{p}3}$ subdivide the interval $(0,t)$ into four subintervals in each of which the appropriate short time and long time GFs for G_X, G_Y and G_Z are to be substituted. Alternatively, when L, W and H do not differ appreciably, we may use a single partition time $\alpha t_\mathrm{p}/L^2$. We now consider the case with a single partition time and show how to optimize it.

As discussed earlier, given a set of truncated short time GFs, we can compute $T^{\mathrm{S}}_{\mathrm{b.c.}}(x,y,z,t)$ for $\alpha t/L^2$ up to $\alpha t_\mathrm{p}/L^2$. For small $\alpha t_\mathrm{p}/L^2$ the error is small but then the computation for $T^{\mathrm{L}}_{\mathrm{b.c.}}(x,y,z,t,t_\mathrm{p})$ requires large number of terms. We wish to determine the optimum t_p i.e., the largest t_p such that $T^{\mathrm{S}}_{\mathrm{b.c.}}(x,y,z,t,t_\mathrm{p})$ remains accurate to prescribed accuracy. A scheme to accomplish this is given below.

We select a sequence $t^{(n)}_\mathrm{p}$ such that $t^{(n+1)}_\mathrm{p} \simeq 2t^{(n)}_\mathrm{p}$, starting with s small t_p. We fix (x,y,z) and some large t (which may be taken as infinity if a steady state solution exists). We compute, either analytically or numerically, the sums

$$T^{\mathrm{S}}_{\mathrm{b.c.}}(x,y,z,t^{(n)}_\mathrm{p}) + T^{\mathrm{L}}_{\mathrm{b.c.}}(x,y,z,t,t^{(n)}_\mathrm{p})$$

as n increases and compare the consecutive sums. For small n the differences between the consecutive sums will be small. As n increases differences between the consecutive sums increase due to errors in the short time contributions (as the error in the long time contribution is controlled). The first n at which the deviation of the sum at $t^{(n+1)}_\mathrm{p}$ from that at $t^{(n)}_\mathrm{p}$ exceeds the prescribed error tolerance determines the optimum t_p given by $t^{(n)}_\mathrm{p}$. It should be noted that the optimum t_p depends on the observation point (x,y,z).

We now present a method by which the optimum partition time may be estimated. Consider a semi-infinite body subject to a step change in temperature at the surface $x = 0$ (the X10B1T0 problem). The solution is given in Eq. (38) with $T_0 = 1$. For an interior point it takes a dimensionless time $\alpha t/x^2 = 0.012$ to cause a temperature rise of one part in 10^{10}. We shall refer to this as the "wave time". For the three-dimensional problem X11B10Y10B00Z11B00B00T0 the solution at (x,y,z) may be approximated by the one-dimensional solution until the two- or three-dimensional effects reach that point. Assuming that $x \leqslant y \leqslant L/2$ and $y \leqslant z$, the distance from (x,y,z) to the nearest boundary is given by $\min(x^2+y^2, x^2+z^2) = x^2+y^2$. We suppose that the speed of propagation of three-dimensional effects is governed by $\alpha t/(x^2+y^2) = 0.012$ and hence $t = 0.012(x^2+y^2)/\alpha = t_1$. Thus the one-dimensional approximation is accurate for $t \leqslant t_1$. and t_1 gives the optimum time t_p at which the solution ceases to be one-dimensional and errors due to three-dimensional effects begin to emerge (see the discussions in Section 4).

3.5. Temperature due to volumetric energy generation and initial condition

The temperature expression for $T_\mathrm{g}(x,y,z,t)$ due to volumetric energy generation given in Eq. (14) may be rewritten as

$$T_g(x,y,z,t) = T_g^S(x,y,z,t), \quad t \leqslant t_p \tag{53}$$

$$T_g(x,y,z,t) = T_g^S(x,y,z,t_p) + T_g^L(x,y,z,t,t_p) \quad t > t_p \tag{54}$$

where

$$T_g^S(x,y,z,t) = \frac{\alpha g_0}{k}\int_{u=0}^{t}\int_{x'=0}^{L} G_X^S(x,x',u)\,dx' \times \int_{y'=0}^{W} G_Y^S(y,y',u)\,dy' \times \int_{z'=0}^{H} G_Z^S(z,z',u)\,dz'\,du \tag{55}$$

$$T_g^L(x,y,z,t,t_p) = \frac{\alpha g_0}{k}\int_{t_p}^{t}\int_{x'=0}^{L} G_X^L(x,x',u)\,dx' \times \int_{y'=0}^{W} G_Y^L(y,y',u)\,dy' \times \int_{z'=0}^{H} G_Z^L(z,z',u)\,dz'\,du \tag{56}$$

With G_X^S given in Eq. (36), G_Y^S given in Eq. (33) and a similar expression for G_Z^S we can carry out the integrations with respect to x', y' and z' in Eq. (55) and obtain

$$T_g^S(x,y,z,t) \simeq \frac{\alpha g_0}{k}\int_{u=0}^{t}(1 - E(x) - E(L-x) - E(y) - E(W-y) - E(Z) - E(H-z))\,du \tag{57}$$

where only low order terms are retained. Carrying out the u-integration then yields

$$T_g^S(x,y,z,t) \simeq \frac{\alpha g_0}{k}\left\{t - 4t(i^2)\operatorname{erfc}\left(\frac{x}{\sqrt{4\alpha t}}\right) + i^2\operatorname{erfc}\left(\frac{L-x}{\sqrt{4\alpha t}}\right) + i^2\operatorname{erfc}\left(\frac{y}{\sqrt{4\alpha t}}\right) + i^2\operatorname{erfc}\left(\frac{W-y}{\sqrt{4\alpha t}}\right) + i^2\operatorname{erfc}\left(\frac{z}{\sqrt{4\alpha t}}\right) + i^2\operatorname{erfc}\left(\frac{H-z}{\sqrt{4\alpha t}}\right)\right\} \tag{58}$$

For definition of $i^2\operatorname{erfc}$ (see [1] or [2]).

Similarly, with the long time GFs given in Eqs. (26)–(28) we can carry out the x'-integration, and substitute into Eq. (56) along with the y'- and z'-integrations in Eqs. (47) and (48) and obtain

$$T_g^L(x,y,z,t,t_p) = \int_{t_p}^{t}\sum_{m=1\,\text{odd}}^{M}\sum_{n=1\,\text{odd}}^{N}\sum_{p=1\,\text{odd}}^{P} \times \exp(-\omega_{mnp}^2\alpha u)\tilde{f}_{mnp}(x,y,z)\,du = \sum_{m=1\,\text{odd}}^{M}\sum_{n=1\,\text{odd}}^{N}\sum_{p=1\,\text{odd}}^{P}\tilde{f}_{mnp}(x,y,z) \times \frac{\exp(-\omega_{mnp}^2\alpha t_p) - \exp(-\omega_{mnp}^2\alpha t)}{\alpha\omega_{mnp}^2} \tag{59}$$

where

$$\tilde{f}_{mnp}(x,y,z) = \frac{64\alpha g_0}{\beta_m\beta_n\beta_p}\sin(\beta_m x/L)\sin(\beta_n y/W) \times \sin(\beta_p z/H) \tag{60}$$

$$\omega_{mnp}^2 = \beta_m^2/L^2 + \beta_n^2/W^2 + \beta_p^2/H^2 \tag{61}$$

An optimum partition time t_p may be obtained using the same scheme in Section 3.4, regardless whether the integrations are done analytically or numerically as in the case when $g(x,y,z,t)$ is not a constant.

Due to more general initial condition the temperature $T_{in}(x,y,z,t)$ is given by Eq. (13). This expression involves integrations with respect to x', y' and z' but not with respect to t. A partition time t_p may be introduced such that the short time and long time GFs are substituted for $t \leqslant t_p$ and $t > t_p$ respectively, resulting in the expressions T_{in}^S and T_{in}^L. An optimum t_p may be obtained by finding the first t_p, as it increases from zero, at which T_{in}^S becomes unequal to T_{in}^L to a prescribed error.

4. Numerical results and discussions

We first consider the temperature $T_{b.c.}$ at the center of a cube with side length L. The steady state temperature there is known to be $T_0/6$. It is seen in Section 3.2 that, given a set of truncated short time GFs, approximations to $T_{b.c.}^S(x,y,z,t)$ can be obtained for short time t up to t_p. One does not know in general, however, the precise errors in such approximations, except that they tend to zero as t_p tends to zero. On the other hand, we see in Section 3.3 that, given a t_p, errors in the long time contribution $T_{b.c.}^L(x,y,z,t,t_p)$ can be controlled by properly restricting the arguments of the exponentials in the series.

Table 1 shows the results for various dimensionless partition times $\alpha t_p/L^2$. These partition times are given in column 1. The second column shows the short time solutions $T_{b.c.}^S(0.5L,0.5L,0.5L,t_p)/T_0$ given by Eq. (3) which increase as $\alpha t_p/L^2$ increases. The fourth column shows the number of terms in the long time computations for $T_{b.c.}^L(0.5L,0.5L,0.5L,\infty,t_p)/T_0$, the results of which are given in column 3. Column 5 gives the sum of columns 2

Table 1
One-dimensional approximation using time partitioning to determine the center, $x = 0.5L$, $y = 0.5L$, $z = 0.5L$, temperature of a cube

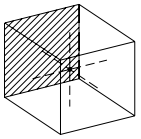

Dimensionless time $\alpha t_p/L^2$	Dimensionless short time solution $T^S_{b.c.}/T_0$	Dimensionless long time solution $T^L_{b.c.}/T_0$	Number of terms for convergence of the long time solution	Sum of short and long time solutions $(T^S_{b.c.} + T^L_{b.c.})/T_0$	True solution $T_{b.c.}/T_0$
0.001	0.0000000000	*0.1666666666	*5950	*0.1666666666	0.0000000000
0.0025	0.0000000000	*0.1666666667	*1499	*0.1666666667	0.0000000000
0.005	0.0000005733	*0.1666660934	*534	*0.1666666667	0.0000005733
0.006	**0.0000050103**	**0.1666616564**	**398**	**0.1666666667**	**0.0000050103**
0.01	*0.0004069520	0.1662600459	184	*0.1666669979	0.0004066209
0.025	*0.0253473187	0.1425826072	45	*0.1679299259	0.0240840595
0.05	*0.1138441966	0.0767761685	17	*0.1906203651	0.0898904982
0.1	*0.2627562698	0.0178042207	7	*0.2805604905	0.1488624461
0.25	*0.4460122207	0.0002098182	1	*0.4462220388	0.1664568486
0.5	*0.4958800056	0.0000001280	1	*0.4958801335	0.1666665388
0.75	*0.5036468697	0.0000000000	1	*0.5036468697	0.1666666667
1	*0.5119291152	0.0000000000	1	*0.5119291152	0.1666666667

The long time solution was truncated when the exponent term reached a magnitude of 20. Entries preceded by an asterisk need not be computed. The bold values represent the optimum partition time.

and 3 and is the steady state solution. Because of the errors in the short time results in column 2, the sum is not constant in column 5, except for t equal to or less than the optimum t_p (which is bold). Column 6 shows the transient temperatures at various $\alpha t/L^2 = \alpha t_p/L^2$ obtained by subtracting column 3 from the optimal steady state values given in column 5. These values are accurate to about 10 decimal places.

We now make some further observations regarding Table 1. For $\alpha t_p/L^2 \leqslant 0.006$, the numerical values for the steady state solution are accurate to nine digits. At larger values of $\alpha t_p/L^2$, the errors are due to the short time contributions. The amount of computation for large time contributions decreases with increasing $\alpha t_p/L^2$. By increasing $\alpha t_p/L^2$ from 0.001 to 0.006, the number of terms needed in the long time series drop from 5950 to 398. Prior to $\alpha t_p/L^2 = 0.006$, the entries in column 3, which are used to obtain the steady state solutions, need not be computed. This is because the steady state results in columns 5 remain the same, independent of t_p for the latter through $\alpha t_p/L^2 \leqslant 0.006$ and thus can be obtained from the entry at $\alpha t_p/L^2 = 0.006$. We shall precede such entries with an asterisk to indicate the fact that they need not be computed. As noted before, transient solutions for $\alpha t_p/L^2 > 0.006$ are given by subtracting column 3 from the steady state solution given in column 5 at $\alpha t_p/L^2 = 0.00$ whereas those for $\alpha t_p/L^2 \leqslant 0.006$ are those given in column 2. We note also that this t_p corresponding to $\alpha t_p/L^2 = 0.006$ plays the role of the optimum t_p discussed in Section 3.4. Rows corresponding to an optimum partition time are bold in the tables. We note that in terms of the estimated optimum partition time t_1 we have $\alpha t_1/L^2 = 0.006$.

We have studied the temperature $T_{b.c.}(x, y, z, t)$ along the centerline $y = 0.5L$, $z = 0.5L$ at different values of x/L and found that as x/L increases, the onset of detectable error in the steady state temperature computations is delayed with time. This is to be expected since the time required for heat to diffuse through the material is inversely proportional to the square of distance. Conversely, once an error becomes measurable in each of the calculations, the magnitude of the error becomes significantly greater, at larger x/L values, for the same dimensionless times. This is due to the edge effects of the parallelepiped, since the point of interest is closer to the $T = 0$ surfaces than to the $T = T_0$ surface with a large value of x/L.

Table 2 shows the temperatures $T_{b.c.}$ in a cube where the observation point (x, y, z) is off the centerline. This causes the side and edge effects of the cube to be much more pronounced. We have the optimal time in this case of $\alpha t_1/L^2 = 0.0015$.

We present in Table 3 the heat flux at the heating surface in the boundary condition case. One interesting

Table 2
One-dimensional approximation using time partitioning to determine the center, $x = 0.25L$, $y = 0.25L$, $z = 0.25L$, temperature of a cube

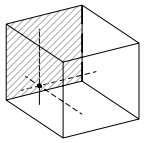

Dimensionless time $\alpha t_p/L^2$	Dimensionless short time solution $T^S_{b.c.}/T_0$	Dimensionless long time solution $T^L_{b.c.}/T_0$	Number of terms for convergence of the long time solution	Sum of short and long time solutions $(T^S_{b.c.} + T^L_{b.c.})/T_0$	True solution $T_{b.c.}/T_0$
0.0005	0.0000000000	*0.3072056232	*33366	*0.3072056232	0.0000000000
0.001	0.0000000227	*0.3072056006	*11722	*0.3072056233	0.0000000226
0.0015	**0.0000050103**	**0.3072006130**	**6365**	**0.3072056233**	**0.0000050103**
0.0025	*0.0004069520	0.3067988368	2940	*0.3072057888	0.0004067864
0.005	*0.0124193307	0.2949398938	1027	*0.3073592245	0.0122657294
0.01	*0.0770998717	0.2358973730	353	*0.3129972448	0.0713082502
0.025	*0.2635524773	0.1070520385	84	*0.3706045158	0.2001535847
0.05	*0.4291952691	0.0371669176	30	*0.4663621868	0.2700387056
0.1	*0.5760594979	0.0067605440	11	*0.5828200420	0.3004450792
0.25	*0.7118079976	0.0000742459	2	*0.7118822435	0.3071313773
0.5	*0.7469179802	0.0000000452	1	*0.7469180255	0.3072055780
0.75	*0.7514071819	0.0000000000	1	*0.7514071819	0.3072056232
1	*0.7553706246	0.0000000000	1	*0.7553706246	0.3072056232

The long time solution was truncated when the exponent term reached a magnitude of 20. Entries preceded by an asterisk need not be computed. The bold values represent the optimum partition time.

Table 3
One-dimensional approximation using time partitioning to determine the dimensionless heat flux in the x direction, at $x = 0$, $y = 0.5L$, $z = 0.5L$, in a cube

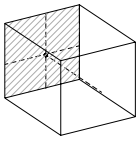

Dimensionless time $\alpha t_p/L^2$	Dimensionless short time solution $q^S_{x\,b.c.}L/kT_0$	Dimensionless long time solution $q^L_{x\,b.c.}L/kT_0$	Number of terms for convergence of the long time solution	Sum of short and long time solutions $(q^S_{x\,b.c.} + q^S_{x\,b.c.})L/kT_0$	True solution $q_{x\,b.c.}L/kT_0$
0.001	17.84124116	*−15.39512228	*11722	*2.44611888	17.84124116
0.0025	11.28379167	*−8.83767280	*2940	*2.44611887	11.28379167
0.003	**10.30064539**	**−7.85452651**	**2251**	**2.44611888**	**10.30064539**
0.005	*7.97884561	−5.53272742	1027	*2.44611819	7.97884630
0.01	*5.64189584	−3.19642463	353	*2.44547121	5.64254351
0.025	*3.56824823	−1.17765461	84	*2.39059362	3.62377349
0.05	*2.52313253	−0.36830740	30	*2.15482513	2.81442628
0.1	*1.78428611	−0.06179511	11	*1.72249100	2.50791399
0.25	*1.16971314	−0.00065997	2	*1.16905317	2.44677885
0.5	*1.01384843	−0.00000040	1	*1.01384802	2.44611928
0.75	*0.99492128	0.00000000	1	*0.99492128	2.44611888
1	*0.97929708	0.00000000	1	*0.97929708	2.44611888

The long time solution was truncated when the exponent term reached a magnitude of 23. Entries preceded by an asterisk need not be computed. The bold values represent the optimum partition time.

Table 4
Three-dimensional approximation with numerical integration using time partitioning to determine the center, $x = 0.5L$, $y = 0.5L$, $z = 0.5L$, temperature of a cube

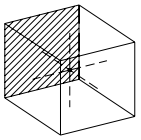

Dimensionless time $\alpha t_p/L^2$	Dimensionless short time solution $T^S_{b.c.}/T_0$	Dimensionless long time solution $T^L_{b.c.}/T_0$	Number of terms for convergence of the long time solution	Sum of short and long time solutions $(T^S_{b.c.} + T^L_{b.c.})/T_0$	True solution $T_{b.c.}/T_0$
0.00500	0.0000005733	*0.1666660934	*1027	*0.1666666667	0.0000005733
0.01000	0.0004066209	*0.1662600459	*353	*0.1666666668	0.0004066208
0.02500	0.0240840593	*0.1425826072	*84	*0.1666666665	0.0240840594
0.05000	**0.0898904982**	**0.0767761685**	**30**	**0.1666666667**	**0.0898904982**
0.10000	*0.1488624431	0.0178042207	11	*0.1666666638	0.1488624460
0.25000	*0.1664519853	0.0002098182	2	*0.1666618035	0.1664568485
0.50000	*0.1666548337	0.0000001280	1	*0.1666549617	0.1666665387
0.75000	*0.1666547890	0.0000000000	1	*0.1666547890	0.1666666667
1.00000	*0.1666547878	0.0000000000	1	*0.1666547878	0.1666666667

The long time solution was truncated when the exponent term reached a magnitude of 20. Entries preceded by an asterisk need not be computed. The bold values represent the optimum partition time.

feature of note in Table 3 is the magnitude of the short and long time solutions at very small dimensionless times. As the dimensionless time tends toward zero, the short time solution tends toward infinity. The long time solution must therefore tend toward negative infinity, since the steady state heat flux at $x = 0$ has a constant value of 2.446118877, and is the sum of the short and long time solutions. This "instability" at very small dimensionless time for the heat fluxes on the heated surface was observed when the maximum exponent was taken to be -20. For the results in Table 3 we have increased the maximum value of the exponent to -23. We mention that, as in the case of temperatures, very accurate transient heat fluxes may be computed from the steady state heat flux in column 5 at small t_p (or for $\alpha t_p/L^2 = 0.0025$ here) and the long time components of the heat fluxes in column 3. Here we have $\alpha t_1/L^2 = 0.003$.

In Table 4 we present more accurate results for the short time temperatures by using Eq. (42) that contains additional terms and carrying out the integrations numerically. The details of the computations are discussed in [5]. It is seen that the short time solutions remain accurate over a larger range of $\alpha t_p/L^2$. This results in a larger optimum t_p corresponding to $\alpha t_p/L^2 = 0.05$ and a decrease in the number of terms in the long time computations from 1027 to 30. It is seen that the estimated optimum partition time based on using t_1 is too conservative and no longer valid when more terms are used in the short time component.

In Tables 5 and 6 we present numerical results for the temperature T_g at the center of a cube and the corresponding heat flux on a face due to a uniform heat generation g_0. The method of time partitioning proceeds similarly as in the boundary condition case. The results in Table 5 for the temperature at the center of a cube due to internal energy generation are comparable to those in Table 1 for the boundary condition case with a same optimum partition time. The heat fluxes on a face of the cube due to internal energy generation given in Table 6 and those due to the heating of a face of the cube given in Table 3 are also similar, with the same optimum partition time.

We finally remark that when the observation point is near a boundary $y = 0$ or $z = 0$ say, t_1 is small and the one-dimensional approximations become invalid quickly. Work is presently in progress to treat such two- or three-dimensional problems effectively.

5. Summary and conclusions

1. Verification of large finite element and control volume codes is supported. This is done by providing a method for finding extremely accurate numerical values for the linear transient heat conduction equation. Temperatures and heat fluxes are both calculated. The geometry of a cube is considered with temperature boundary conditions on all six surfaces. The classical method of separation of variables builds the solution

Table 5
One-dimensional approximation using time partitioning to determine the center, $x = 0.5L$, $y = 0.5L$, $z = 0.5L$, temperature of a cube with volume energy generation

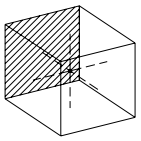

Dimensionless time $\alpha t_p/L^2$	Dimensionless short time solution kT_g^S/g_0L^2	Dimensionless long time solution kT_g^L/g_0L^2	Number of terms for convergence of the long time solution	Sum of short and long time solutions $k(T_g^S + T_g^L)/g_0L^2$	True solution kT_g/g_0L^2
0.0025	0.0025000000	*0.0537128298	*1875	*0.0562128298	0.0025000000
0.005	0.0049999988	*0.0512128310	*642	*0.0562128298	0.0049999988
0.006	**0.0059999858**	**0.0502128440**	**486**	**0.0562128298**	**0.0059999858**
0.01	*0.0099971115	*0.0462157170	229	*0.0562128285	0.0099971128
0.025	*0.0241548870	*0.0320325043	51	*0.0561873913	0.0241803255
0.05	*0.0388948227	*0.0157789947	20	*0.0546738174	0.0404338351
0.1	*0.0306960026	*0.0036088667	7	*0.0343048692	0.0526039632
0.25	*−0.1697883407	*0.0000425180	1	*−0.1697458227	0.0561703118
0.5	*−0.7578355602	*0.0000000259	1	*−0.7578355342	0.0562128039
1	*−2.2947756723	*0.0000000000	1	*−2.2947756723	0.0562128298

The long time solution was truncated when the exponent term reached a magnitude of 20. Entries preceded by an asterisk need not be computed. The bold values represent the optimum partition time.

Table 6
One-dimensional approximation using time partitioning to determine the dimensionless heat flux in the x direction, at $x = 0$, $y = 0.5L$, $4z = 0.5L$, in a cube with volume energy generation

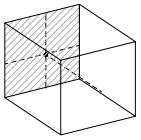

Dimensionless time $\alpha t_p/L^2$	Dimensionless short time solution $q_{x\,b.c.}^S L/kT_0$	Dimensionless long time solution $q_{x\,b.c.}^L L/kT_0$	Number of terms for convergence of the long time solution	Sum of short and long time solutions $(q_{x\,b.c.}^S + q_{x\,b.c.}^S)L/kT_0$	True solution $q_{x\,b.c.}L/kT_0$
0.001	−0.0356824823	*−0.2461908319	*7268	*−0.2818733142	−0.0356824823
0.0025	−0.0564189584	*−0.2254543559	*1875	*−0.2818733142	−0.0564189584
0.003	**−0.0618038723**	**−0.2200694419**	**1388**	**−0.2818733142**	**−0.0618038723**
0.005	*−0.0797884561	−0.2020848645	642	*−0.2818733206	−0.0797884497
0.01	*−0.1128379167	−0.1690468831	229	*−0.2818847999	−0.1128264311
0.025	*−0.1784120559	−0.1056567135	51	*−0.2840687694	−0.1762166008
0.05	*−0.2521785811	−0.0499182734	20	*−0.3020968546	−0.2319550408
0.1	*−0.3528821768	−0.0113391240	7	*−0.3642213008	−0.2705341902
0.25	*−0.5139350419	−0.0001335744	1	*−0.5140686163	−0.2817397398
0.5	*−0.6312536196	−0.0000000815	1	*−0.6312537011	−0.2818732327
1	*−0.7290967103	0.0000000000	1	*−0.7290967103	−0.2818733142

The long time solution was truncated when the exponent term reached a magnitude of 23. Entries preceded by an asterisk need not be computed. The bold values represent the optimum partition time.

from two parts, steady state and transient. However, in the classical steady state solution given by Carslaw and Jaeger [3], the computed heat flux at the heated surface oscillates through positive and negative values as more terms in the summations are included. In contrast, the proposed method gives extremely accurate

values (to 9 or more significant figures) without oscillation.

2. The example of a cube with temperature boundary conditions is treated but the method can be employed for a parallelepiped with heat flux and convective boundary conditions in the same manner.

3. New insights are given for the calculation of the steady state component, which is usually the most difficult part.

4. A criterion is presented for determining the duration for the two- and three-dimensional effects to affect the solution. This criterion is based on an accuracy of one part in 10^{10} but can be made more or less if desired. The criterion is $\alpha t/(x^2+y^2) = 0.012$ where x and y are less than z and $x < L/2$ and $y < W/2$. With this method the extra computation to generate values with errors about one part in 10^9 is less than a factor of 10 than that required for error of one part in 10,000. This contrasts significantly with the additional effort required to reduce errors using the finite element method, for example. Such accurate results are not much more than for errors several magnitudes greater, unlike for finite element methods.

5. The method avoids numerical integration for much of the body, unlike the time partitioning method of Ref. [5]. Such integration is implicit in the method. However, without some extensions the proposed method herein cannot avoid numerical integration for points near the corners and edges. Such extensions are under development and may be the subject of future papers.

Acknowledgements

The research reported here has been supported in part by a contract by the U.S. Department of Energy, administered by the Sandia National Laboratory in Albuquerque, New Mexico. We wish to thank Dr. Kevin J. Dowding, Program Monitor, for his encouragement.

References

[1] S. Abramowitz, I.A. Stegun, Handbook of Mathematical Functions, Dover Publications, Inc, New York, 1965.
[2] J.V. Beck, K.D. Cole, A. Haji-Sheikh, B. Litkouhi, Heat Conduction Using Green's Functions, Hemisphere Press, Washington, DC, 1992.
[3] H.S. Carslaw, J.C. Jaeger, Conduction of Heat in Solids, second ed., Oxford University Press, 1959.
[4] C.M. Linton, Rapidly convergent representations for Green's functions for Laplace's equation, Proc. Royal Soc. London A 455 (1999) 1767–1797.
[5] R.L. McMasters, K.J. Dowding, J.V. Beck, D.H.Y. Yen, Methodology to generate accurate solutions for verification in transient three-dimensional heat conduction. J. Numer. Heat Transfer, Part B, 41 (2002).
[6] R.L. McMasters, Z. Zhou, K.J. Dowding, C. Somerton, J.V. Beck, Exact solution for nonlinear thermal diffusion and its use for verification. AIAA J. Thermalphys. Heat Transfer 16 (2) (2002).
[7] M.N. Ozisik, Heat Conduction, Wiley, New York, 1980.
[8] J. Strain, Fast potential theory. II. Layer potentials and discrete sums, J. Comput. Phys. 99 (1992) 251–270.